ELEMENTA
Science of the Anthropocene

Kahru, M, et al. 2021. Satellite detection of dinoflagellate blooms off California by UV reflectance ratios. *Elem Sci Anth*, 9: 1. DOI: https://doi.org/10.1525/elementa.2020.00157

RESEARCH ARTICLE

Satellite detection of dinoflagellate blooms off California by UV reflectance ratios

Mati Kahru[1,*], Clarissa Anderson[2], Andrew D. Barton[1,3], Melissa L. Carter[1], Dylan Catlett[4], Uwe Send[1], Heidi M. Sosik[5], Elliot L. Weiss[1], and B. Greg Mitchell[1]

As harmful algae blooms are increasing in frequency and magnitude, one goal of a new generation of higher spectral resolution satellite missions is to improve the potential of satellite optical data to monitor these events. A satellite-based algorithm proposed over two decades ago was used for the first time to monitor the extent and temporal evolution of a massive bloom of the dinoflagellate *Lingulodinium polyedra* off Southern California during April and May 2020. The algorithm uses ultraviolet (UV) data that have only recently become available from the single ocean color sensor on the Japanese GCOM-C satellite. Dinoflagellates contain high concentrations of mycosporine-like amino acids and release colored dissolved organic matter, both of which absorb strongly in the UV part of the spectrum. Ratios <1 of remote sensing reflectance of the UV band at 380 nm to that of the blue band at 443 nm were used as an indicator of the dinoflagellate bloom. The satellite data indicated that an observed, long, and narrow nearshore band of elevated chlorophyll-a (Chl-a) concentrations, extending from northern Baja to Santa Monica Bay, was dominated by *L. polyedra*. In other high Chl-a regions, the ratios were >1, consistent with historical observations showing a sharp transition from dinoflagellate- to diatom-dominated waters in these areas. UV bands are thus potentially useful in the remote sensing of phytoplankton blooms but are currently available only from a single ocean color sensor. As several new satellites such as the NASA Plankton, Aerosol, Cloud, and marine Ecosystem mission will include UV bands, new algorithms using these bands are needed to enable better monitoring of blooms, especially potentially harmful algal blooms, across large spatiotemporal scales.

Keywords: Remote sensing, Ocean color, Dinoflagellates, Harmful algal blooms, California Current Ecosystem, Plankton

1. Introduction

Dinoflagellate blooms are common off the coast of California, particularly in the Southern California Bight (Venrick, 2002; Anderson et al., 2008; Barron et al., 2014; Catlett and Siegel, 2018). Dinoflagellates tend to accumulate and "bloom" as the water column stratifies following the relaxation of upwelling or significant precipitation and freshwater discharge events (Venrick, 2002; Anderson et al., 2008; Mantyla et al., 2008; Barth et al., 2020; Fischer et al., 2020). Upwelling-relaxation conditions are typical of spring, summer, and early fall in the Southern California Bight (Mantyla et al., 2008) and may be more common in the California Current System (CCS) during the negative phase of the North Pacific Gyre Oscillation (NPGO), which seems to favor dinoflagellates over diatoms on a roughly decadal cycle (Fischer et al., 2020; Catlett et al., n.d.). The so-called age of dinoflagellates (Jester et al., 2009; Fischer et al., 2020) linked to the warm phase of the NPGO is associated with a higher incidence of dinoflagellate-dominated harmful algal blooms (HABs) that are anticipated to increase in occurrence as climate changes in the CCS (Fischer et al., 2020).

A very common bloom-forming dinoflagellate in the CCS is *Lingulodinium polyedra* (F. Stein) J. D. Dodge, 1989 (formerly *Gonyaulax polyedra*; by many authors *Lingulodinium polyedrum*, e.g., Stires and Latz, 2018). *L. polyedra* blooms not only produce spectacular and episodic bioluminescent displays by night in Central and Southern California but are often characterized by brown or red water in the nearshore when growing at high biomass (Allen, 1938). They are thus often referred to by the common moniker "red tide."

Monitoring the initiation and offshore extent of phytoplankton blooms is difficult as few instruments are

[1] Scripps Institution of Oceanography, University of California San Diego, La Jolla, CA, USA
[2] Southern California Coastal Ocean Observing System, Scripps Institution of Oceanography, University of California San Diego, La Jolla, CA, USA
[3] Section of Ecology, Behavior and Evolution, University of California San Diego, La Jolla, CA, USA
[4] Interdepartmental Graduate Program in Marine Science, University of California, Santa Barbara, CA, USA
[5] Woods Hole Oceanographic Institution, Woods Hole, MA, USA
* Corresponding author:
Email: mkahru@ucsd.edu

currently deployed to capture in situ bloom initiation outside of several nearshore pier locations with weekly HAB monitoring (Kudela et al., 2015), and currently, there is no generalized method of remote detection by satellite. In situ optical measurements during a large bloom of *L. polyedra* in 1995 (Kahru and Mitchell, 1998) showed that the bloom had very strong absorption of ultraviolet (UV) light. Separately, Vernet and Whitehead (1996) and Whitehead and Vernet (2000) demonstrated that high concentrations of UV-absorbing mycosporine-like amino acids (MAAs) in both particulate and dissolved organic matter were associated with the *L. polyedra* bloom and lab cultures. MAAs are small molecules that absorb radiation in the UVA and UVB region but have very low absorption in the visible range (Shick and Dunlap, 2002). The absorption maxima in the 300–400 nm range are modulated by the conjugation of varying amino acids or amino alcohols to a cyclohexenone or cyclohexenimine chromophore. MAAs diminish the deleterious effects of UV radiation by acting as a sunscreen and confer varying degrees of antioxidant protection to phytoplankton (Moisan and Mitchell, 2001; Shick and Dunlap, 2002). MAAs may therefore provide competitive advantage to phytoplankton capable of MAA synthesis, as species with lower UV sensitivity may outcompete others in the high light in near-surface environments, favoring bloom formation (Carreto et al., 2018).

While MAAs are present in many phytoplankton taxa, there is significant variability in MAA composition between species. *L. polyedra* has previously been shown to contain the MAAs mycosporine-glycine, shinorine, porphyra, mycosporine-glycine-valine, palythine, and palythene and is capable of not only synthesizing these MAAs but also excreting them into seawater (Vernet and Whitehead, 1996; Whitehead and Vernet, 2000). While the majority of these molecules absorb maximally below 340 nm, palythene absorbs maximally at 362 nm and the spectral signature extends into the 380 nm wave band. In situ measurements during the 1995 bloom (Kahru and Mitchell, 1998) showed that the increased UV absorption resulted in reduced remote sensing reflectance (R_{rs}, sr^{-1}) in the UV, whereas in the blue and other bands, reflectance followed a relationship with chlorophyll-a (Chl-a) that was similar to that in typical phytoplankton assemblages in the California Current Ecosystem (**Figure 1**). Therefore, the $R_{rs}380/R_{rs}443$ ratio can be used to discriminate *L. polyedra* blooms from other common bloom-forming species in the Southern California Bight such as Pseudo-nitzschia spp. An $R_{rs}380/R_{rs}443$ ratio < 1 may be considered an indicator of an *L. polyedra* bloom with high concentration of MAAs, whereas $R_{rs}380/R_{rs}443 > 1$ is likely an indicator of a bloom dominated by diatoms. Kahru and Mitchell (1998) showed that the reduced $R_{rs}380/R_{rs}443$ ratio was able to distinguish a dinoflagellate-dominated phytoplankton community at Chl-a concentrations greater than approximately 1–2 mg m^{-3} (**Figure 1**). Subsequently, the "red tide index" (Mitchell and Kahru, 2009) using the reduced UV reflectance in red tides was proposed for the Global Imager (GLI), which was the first ocean color satellite sensor with a 380 nm band. Unfortunately, the GLI mission was short due to a technical failure, but the Second-Generation Global Imager (SGLI) on GCOM-C satellite (Tanaka et al., 2018) has been collecting $R_{rs}380$ data since early 2018.

Here, we demonstrate the capability to apply the UV-to-blue reflectance ratio to newly available satellite data from the SGLI. In April–May 2020, a large and unprecedented bloom of *L. polyedra* occurred and spanned the nearshore zone of the entire Southern California Bight to northern Baja. The high biomass and prolonged duration led to massive fish and invertebrate die-offs, suggesting that the potential for *L. polyedra* blooms to produce toxins should be considered. SGLI composite observations over this time period showed a long, narrow nearshore band of elevated Chl-a concentrations extending from northern Baja to

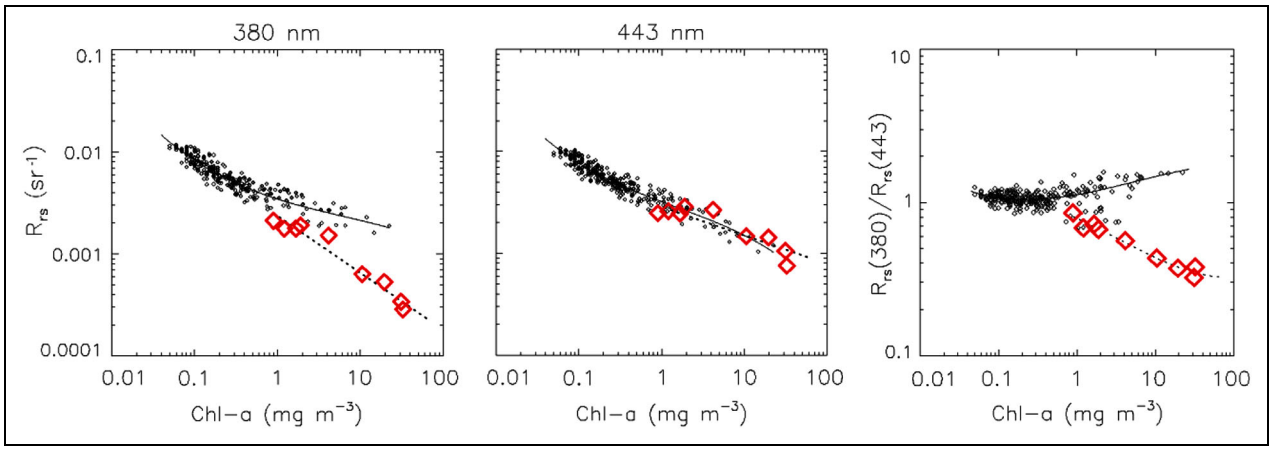

Figure 1. Remote sensing reflectance at 380 and 443 nm and their ratio as functions of chlorophyll-a (Chl-a). Remote sensing reflectance, R_{rs} (sr^{-1}), at 380 and 443 nm and their ratio, R_{rs} (380)/R_{rs}(443), as functions of Chl-a measured in situ (data from Kahru and Mitchell, 1998) from a bloom of *Lingulodinium polyedra* (large, open red diamonds) and from typical phytoplankton assemblages in the California Current Ecosystem sampled during CalCOFI cruises (small, open black diamonds). The solid line is a polynomial fit to the CalCOFI data, and the dotted line is a linear fit to the bloom data. DOI: https://doi.org/10.1525/elementa.2020.00157.f1

Santa Monica Bay. This band was accompanied by $R_{rs}380/R_{rs}443$ values <1, suggesting dominance by *L. polyedra*. The bloom apparently did not extend further north into the Santa Barbara Channel (SBC) where high Chl-a concentration was also evident but $R_{rs}380/R_{rs}443$ values were >1, in agreement with historical observations showing a sharp transition from dinoflagellate- to diatom-dominated waters in this area. Our observations confirm that the $R_{rs}380/R_{rs}443$ band ratio can discriminate blooms with high UV absorption, such as *L. polyedra* blooms, from other phytoplankton assemblages and suggest potential for future satellite ocean color sensors equipped with UV bands to monitor dinoflagellate blooms across large spatiotemporal scales.

2. Methods

2.1. In situ data

Collection of in situ data during the *L. polyedra* bloom in April–May 2020 was limited due to the restrictions imposed by the COVID-19 pandemic. However, monitoring by the Harmful Algal Bloom Monitoring and Alert Program (HABMAP; supported by the Southern California Coastal Ocean Observing System) was conducted weekly at Scripps and Santa Monica Piers, but not at Newport Pier or Stearns Wharf. HABMAP sampling for chlorophyll and cell counts is detailed in Hatch et al. (2013) and was sustained at Scripps Pier given the strong collaboration with the California Department of Public Health and the need to alert the State of California about HABs.

Bloom initiation and development was also captured by a coincident deployment of an Imaging FlowCytobot (IFCB; Olson and Sosik, 2007; McLane Research Laboratories, Inc.) on the Del Mar mooring (32.93°N; 117.317°W) near San Diego. The IFCB takes images of particles and plankton in a known volume of water and therefore can be used to estimate the abundance of *L. polyedra* and other taxa through time. The mooring is approximately 5 km offshore on the 100-m isobath, and the instrument was mounted on the mooring wire at approximately 5-m depth. The IFCB was configured with both chlorophyll fluorescence and light scattering signals triggering acquisition of high-resolution (approximately 1 μm) images of plankton and other particles in 5 mL of seawater sampled 4–12 times per day during the deployment on the mooring. This process resulted in over 900,000 images collected in the first 6 months of 2020. IFCB images were analyzed according to the methods outlined in Sosik and Olson (2007), but with updated analysis code (Sosik et al., 2020) and with the support vector machine replaced by a convolutional neural network classifier. IFCB products are available at https://ifcb-data.whoi.edu/SIO_Delmar_mooring. The concentration of *L. polyedra* was estimated from classifier output (intermittently verified by manual inspection of images) and the volume of seawater imaged by IFCB. For comparison with the satellite data products, daily concentration estimates were produced by pooling all samples by day (total cell count divided by total volume of seawater imaged for a given day).

2.2. Satellite data

The GCOM-C satellite (Tanaka et al., 2018) with the SGLI was launched in late 2017, and the data since early 2018 are available at the G-Portal website: https://gportal.jaxa.jp/gpr/. Atmospheric correction of satellite ocean color data is complicated, particularly in the UV and blue regions. Improved atmospheric correction (Toratani et al., 2020) implemented in the Version 2.0 reprocessing is therefore critical for producing high-quality data. Version 2.0 SGLI Level-2 data sets (i.e., calibrated and navigated swath data) at 1-km and 250-m resolutions were mapped, respectively, to 1-km and 250-m grids covering the Central and Southern California coast. Data sets of Chl-a using the SGLI standard algorithm (Murakami, 2020) and remote sensing reflectance (R_{rs}, sr^{-1}) at multiple wavelength bands were extracted, and various band ratios were calculated. Pixels with no or low-quality data (identified with flags DATAMISS, LAND, CLDICE, CLDAFFCTD, NEGNLW, and ATM-METHOD) were eliminated. Additionally, cloud masks were expanded to eliminate cloud-edge pixels.

To put the 2020 bloom into perspective, we used a multisatellite Chl-a time series composited over the period 1996–2020 (http://spg-satdata.ucsd.edu/ca1km/). Several techniques were applied to reduce the effect of missing data due to clouds and to produce a continuous time series with a 5-day temporal resolution. First, daily data sets were created by merging data from multiple sensors and then 5-day running mean operation was applied to the daily data sets. Five-day composites were created, and missing pixels were filled by linear interpolation. The following sensors were used in the multisatellite time series: OCTS (1996–1997), SeaWiFS (1997–2010), MODIS-Terra (2000–present), MERIS (2002–2012), MODIS-Aqua (2002–2020), VIIRS-SNPP (2012–present), OLCI-A (2017–present), OLCI-B (2019–present), and VIIRS-JPSS1 (2019–present). For comparisons with in situ time series, we extracted the mean Chl-a from a circle with a diameter of 10 km centered at the in situ station. When the station was a pier, the satellite sampling in a 10-km circle (semicircle at best) was inherently biased to the low side as it was based on predominantly offshore pixels with lower concentrations.

3. Results and discussion

3.1. L. polyedra *bloom in April—May 2020*

A time series of multisatellite Chl-a for a circle with 10 km diameter centered at the Del Mar mooring site (**Figure 2A**) shows the *L. polyedra* bloom as a distinct maximum in Chl-a from mid-April to the end of May 2020 with maximum Chl-a concentrations over 18 mg m^{-3}. This maximum is the average of valid approximate 1 km^2 pixels in the 10-km circle area. The maximum Chl-a concentration in April–May 2020 was the highest since the start of satellite data in November 1996. The second highest concentration (>15 mg m^{-3}) was on December 1, 2010 (not shown), with a total of nine blooms exceeding 10 mg m^{-3} at this site. As the location of the mooring is in a high-gradient zone of Chl-a from coast to offshore (the location of the mooring is shown in **Figure 3**), the retrieved Chl-a concentrations are therefore sensitive to

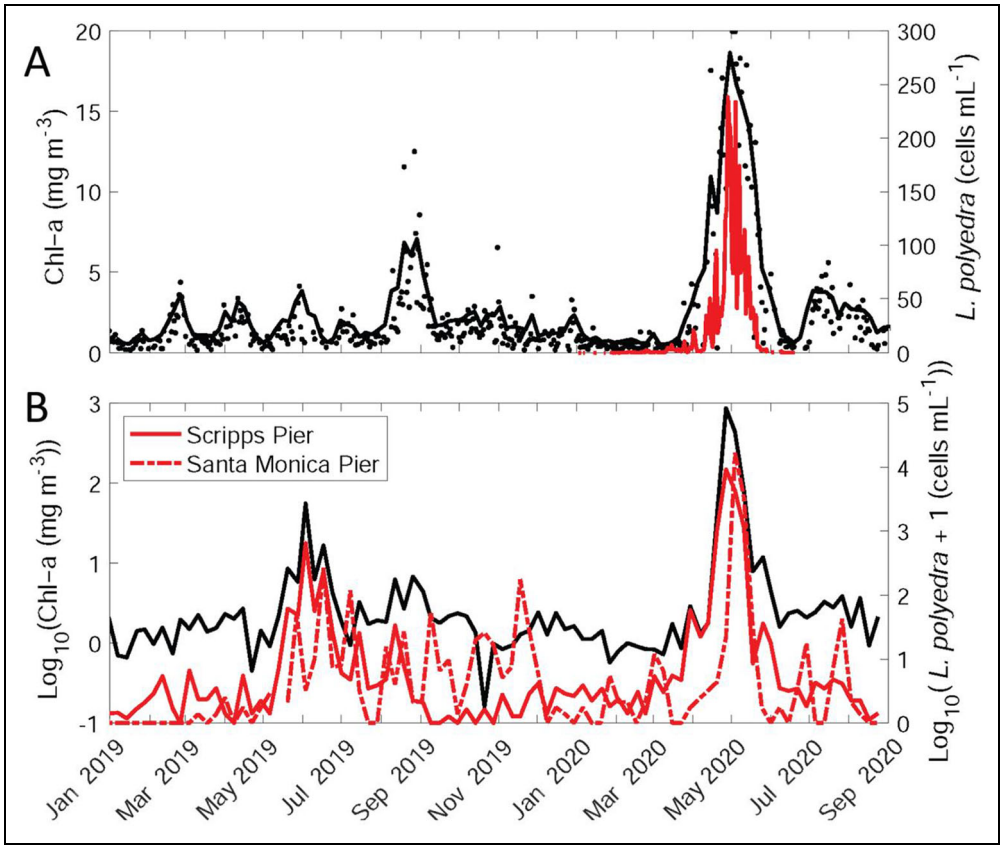

Figure 2. Mean satellite-derived chlorophyll-a (Chl-a) concentrations and cell concentrations. (A) Multisatellite-derived Chl-a concentration (black, left axis) in a circle of 10 km diameter centered at the Del Mar mooring from daily images (dots) and 5-day composites (black line). Daily average concentrations of *Lingulodinium polyedra* cells (red line, right axis) from Imaging FlowCytobot images at the mooring. (B) Multisatellite Chl-a at Scripps Pier (black line, left axis) and concentrations of *L. polyedra* cells (red, right axis) counted manually at SIO Pier (solid red line, right axis) and at the Santa Monica Pier (dashed red line, right axis). A pseudocount of 1 cell mL^{-1} was added to *L. polyedra* concentrations prior to the log transformation to prevent undefined values. DOI: https://doi.org/10.1525/elementa.2020.00157.f2

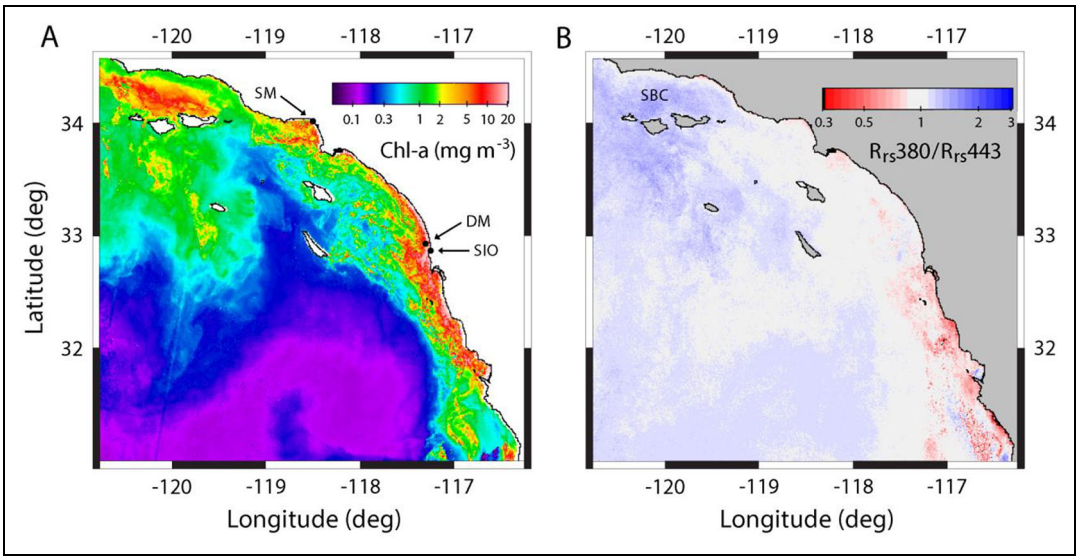

Figure 3. Chlorophyll-a (Chl-a) concentrations and $R_{rs}380/R_{rs}443$ ratios from Second-Generation Global Imager (SGLI) satellite data during the bloom. (A) Chl-a and (B) $R_{rs}380/R_{rs}443$ off Southern California during the period of April 7–May 24, 2020, corresponding to the peak in Chl-a in **Figure 1**. Both panels were created using SGLI 250 m Version 2.0 satellite data. The arrows show the locations of the Santa Monica Pier, Del Mar mooring (DM), and Scripps Pier (SIO). The Santa Barbara Channel is shown in B. DOI: https://doi.org/10.1525/elementa.2020.00157.f3

availability of individual satellite pixels, particularly near the coast.

The daily-binned time series of *L. polyedra*, observed by the IFCB deployed at the Del Mar mooring (**Figure 2A**), showed a dramatic maximum that corresponded well temporally with the satellite-derived Chl-a peak. The duration of the bloom identified by IFCB *L. polyedra* cell counts was shorter (from approximately April 10 to May 20) than the Chl-a maximum observed in satellite data (March 30–May 29 with mean Chl-a > 3 mg m^{-3}). As daily Chl-a values correspond well to the 5-day composites (**Figure 2A**), we conclude that the longer duration of the satellite-derived Chl-a bloom was caused by spatial averaging of the patchy distributions in the 10 km circle. Chl-a time series constructed from values of a single pixel nearest to the mooring showed a peak duration that was comparable to that of in situ IFCB data, albeit with many missing values and more variability. Notably, IFCB observations approximately every 2 h during the bloom period showed high levels of patchiness in *L. polyedra* concentrations, with daily maxima commonly >3-fold and some days >5-fold above the daily mean. For several days in late April and early May, daily maxima at the Del Mar mooring exceeded 1,000 cells mL^{-1}.

Weekly sampling at the Scripps and Santa Monica Piers (**Figure 2B**) showed that the *L. polyedra* bloom occurred at approximately the same time but at drastically higher magnitudes than observed at the off shore Del Mar mooring. At Scripps Pier, *L. polyedra* concentrations reached their maximum observed values of 9,170 cells mL^{-1} on April 27, 2020, and were found at concentrations >1,000 cells mL^{-1} in weekly samples from April 20 to May 11, 2020. These observations coincided with Chl-a concentrations >40 mg m^{-3} and as high as 867 mg m^{-3} (also on April 27, 2020) and roughly corroborate the duration of the bloom at Del Mar observed by IFCB, though the high-frequency sampling resolution offered by IFCB provides a finer temporal-scale estimate of the duration of the bloom. Further north at Santa Monica Pier, *L. polyedra* concentrations reached a maximum of 16,800 cells mL^{-1} on May 4, 2020, were found at 3,400 cells mL^{-1} a week later and declined to approximately 30 cells mL^{-1} on May 18. The bloom duration was also apparently shorter at Santa Monica Pier relative to Scripps Pier, with *L. polyedra* concentrations >1,000 cells mL^{-1} observed in two consecutive weekly samples at Santa Monica compared to four consecutive weekly samples at Scripps. Notably, the *L. polyedra* concentrations observed at Scripps and Santa Monica Piers were approximately 50-fold higher than those observed by IFCB at the Del Mar mooring, corroborating the pattern of increasing bloom magnitude from nearshore to offshore waters shown in satellite imagery (**Figures 3** and **4**).

Compared to the merged sensor data set (e.g., Chl-a in **Figure 2A**), data from a single sensor such as SGLI have considerably less coverage due to orbital characteristics and cloud cover during overpasses. We were able to acquire 17 SGLI scenes during the period of April 7–May 24 covering the April–May bloom (**Figure 3**). Composites over this time period were calculated as averages over valid pixels for Chl-a but as medians over valid pixels for the $R_{rs}380/R_{rs}443$ ratio. (Median compositing is needed for ratios as the mean is biased relative to the expectation. For example, the mean of ratios 2 and 0.5 is not 1.) The spatial distribution of Chl-a (**Figure 3A**) shows high values along a coastal band, particularly off Southern California, and a separate high Chl-a area to the north in the SBC. The decreased $R_{rs}380/R_{rs}443$ ratios in the Southern California coastal areas (**Figure 3B**) of high Chl-a is likely due to the dinoflagellate bloom with low UV reflectance caused by the high MAA absorption. On the other hand, the high Chl-a area in the SBC accompanied by high $R_{rs}380/R_{rs}443$

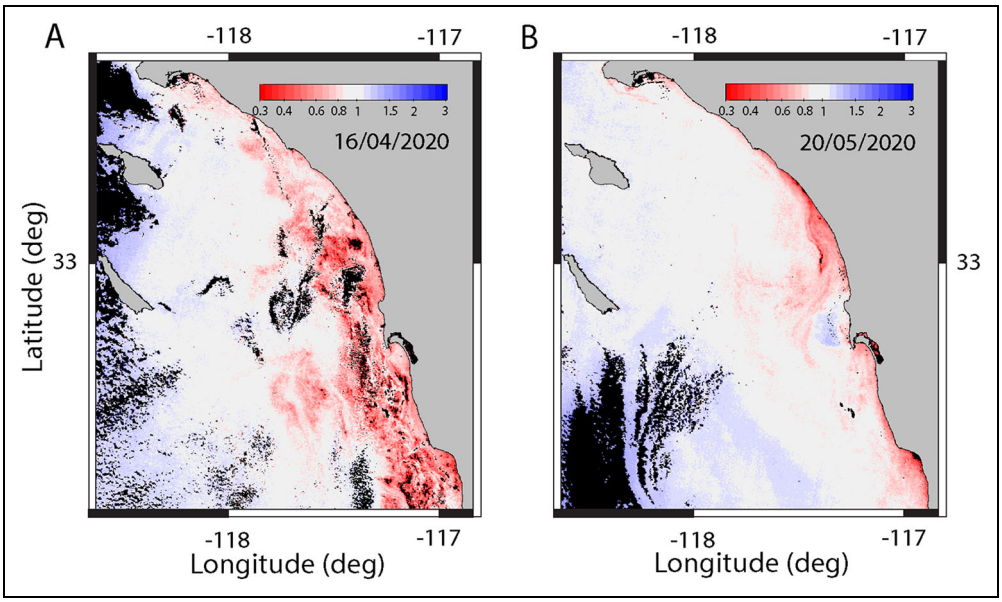

Figure 4. Examples of the $R_{rs}380/R_{rs}443$ ratio images. Examples of the $R_{rs}380/R_{rs}443$ ratios on April 16 (A) and May 20 (B) in 2020. Both panels were created using Second-Generation Global Imager 250 m Version 2.0 satellite data. Black areas have no valid data due to clouds. DOI: https://doi.org/10.1525/elementa.2020.00157.f4

ratios is probably associated with a different phytoplankton community, most likely dominated by diatoms, typical of the upwelling domain adjacent to Point Conception. Offshore areas with lower Chl-a showed the $R_{rs}380/R_{rs}443$ ratio slightly above 1 indicating fewer dinoflagellates. Atmospheric correction of SGLI UV and blue bands is difficult (Toratani et al., 2020), and uncertainties in R_{rs} are probably significant. Quantifying error in the $R_{rs}380/R_{rs}443$ ratio is currently difficult, so we assume that values close to 1 (i.e., white pixels in **Figure 3B**) cannot be classified as indicating either dinoflagellate (ratio < 1) or other phytoplankton (ratio > 1; e.g., diatom-dominated). Band ratios, however, are expected to have reduced errors compared to single band R_{rs}, as over- and underestimation typically correlate positively for adjacent bands.

3.2. Qualitative validation of L. polyedra *bloom detection*

Individual SGLI scenes that were used to create the $R_{rs}380/R_{rs}443$ composite (**Figure 3B**) were quite fragmented due to frequent cloud cover. The overpass time of the SGLI sensor is approximately 10:30 local time and may therefore be biased due to the significant diurnal vertical migration of dinoflagellates resulting in strong temporal changes in surface water. Individual images also show high spatial and temporal variability in $R_{rs}380/R_{rs}443$ (**Figure 4**). This kind of variability is expected due to both real processes, such as diurnal changes associated with vertical migration of dinoflagellates and the synthesis of MAAs; vertical mixing of the bloom by wind events; internal waves; and so on; and errors in atmospheric correction. Future work should concentrate on validation of the SGLI R_{rs} values and band ratios, particularly of the 380 nm band based on high-quality in situ measurements.

While in situ observations to validate the extent of the *L. polyedra* bloom are sparse, particularly as the bloom occurred during COVID-19 pandemic shelter-in-place orders, those available at the Del Mar mooring and at Scripps and Santa Monica Piers confirm the large magnitude and timing of the bloom and suggest that the broad spatial patterns in bloom extent inferred by satellite are reasonable (**Figure 2**). The April–May composite of Chl-a concentrations showed a nearshore band of anomalously high Chl-a values centered on Scripps Pier, with both the Del Mar mooring and Santa Monica Pier located outside this band. While in situ Chl-a observations are not available at Santa Monica, Chl-a concentrations at Scripps Pier were more than an order of magnitude higher than the maximum satellite chlorophyll concentrations observed at the Del Mar mooring. Similarly, peak *L. polyedra* concentrations at Scripps and Santa Monica Piers were approximately 50-fold higher than those observed at the Del Mar mooring. While all three sites were associated with the "red" false color in **Figure 3** ($R_{rs}380/R_{rs}440 < 1$) in April–May on average, the April–May composite image showed a decrease in $R_{rs}380/R_{rs}440$ (a "reddening" of surface waters) from offshore to onshore, in line with the increase in *L. polyedra* at Scripps Pier relative to Del Mar (**Figures 2** and **3**). Finally, the mechanism(s) driving the shorter duration and delayed timing of the bloom at Santa Monica Pier relative to Scripps Pier are unknown. However, these observations suggest that the occurrence of "red" waters in the Southern California Bight increases further south in the Bight, as shown in both the $R_{rs}380/R_{rs}440$ and Chl-a composite and single-day images (**Figures 2–4).**

Previous studies in the Southern California Bight and SBC also suggest that the observed extent of the bloom (**Figure 3**) is realistic. *L. polyedra* blooms are common in coastal waters from northern Baja to Santa Monica Bay (Allen, 1938; Goodman et al., 1984; Goericke, 2011; Taylor et al., 2015), as observed here. However, past observations in the SBC have found sharp gradients in sea-surface temperature and chlorophyll concentrations, transitioning from warmer and more oligotrophic waters in the northern and eastern SBC to colder productive waters in the southern and western SBC (Otero and Siegel, 2004; Henderikx Freitas et al., 2017). These gradients in SST and chlorophyll concentrations are accompanied by gradients in the dominant phytoplankton groups, as diatoms are overwhelmingly dominant in the upwelling-impacted waters of the SBC, while dinoflagellates tend to become more dominant in the warmer, more stratified waters further south in the Bight (Venrick, 2002; Anderson et al., 2006, 2008; Taylor et al., 2015; Catlett et al., n.d.). These patterns are particularly pronounced in the spring and early summer when the combination of the reduced upwelling and enhanced entrainment of upwelling-impacted CCS waters in the western and southern SBC favors more pronounced diatom blooms in this region relative to further south (Harms and Winant, 1998; Henderikx Freitas et al., 2017; Catlett et al., n.d.). Thus, the high $R_{rs}380/R_{rs}443$ values observed in April–May 2020 in the SBC are likely accurate in their discrimination of a diatom-dominated bloom in response to more intense upwelling, while the low $R_{rs}380/R_{rs}443$ values south of Santa Monica Bay accurately portray the extent of the historic 2020 *L. polyedra* bloom (**Figure 3**).

3.3. Implications for future satellite ocean color sensors

UV absorption by MAAs in both the dissolved and particulate phases has been documented in coastal California (Vernet and Whitehead, 1996; Whitehead and Vernet, 2000; Barron et al., 2014), and its impact on above-water reflectance has been implied (Kahru and Mitchell, 1998). While MAAs are not unique to *L. polyedra*, or even dinoflagellates, observations in the Southern California Bight coupled with the results presented above indicate that enhanced UV absorption driven by MAAs is associated with elevated dinoflagellate abundances (Kahru and Mitchell, 1998; Barron et al., 2014). *L. polyedra* has long been recognized as one of the most prominent bloom-forming dinoflagellates in the Southern California Bight (Allen, 1938; Goodman et al., 1984), and thus elevated UV absorption will often correspond to *L. polyedra* concentrations in this region. However, satellite observations should continue to be paired with in-water observations of the phytoplankton community, as the composition of

phytoplankton communities and the dominant bloom-forming species may change under future climate scenarios.

The $R_{rs}380/R_{rs}443$ band ratio approach applied to the historic *L. polyedra* bloom in April–May 2020 produced a reasonable spatial pattern and duration of the bloom not afforded by any other currently available ocean observing technology. Because the SGLI is currently the only ocean color sensor with a 380 nm band, and its UV products are still under development, this work is the first practical application of the method using satellite data. NASA's upcoming Plankton, Aerosol, Cloud, and marine Ecosystem (PACE) mission will be equipped with an ocean color instrument capable of resolving $R_{rs}(\lambda)$ every 5 nm from 340 to 885 nm (Werdell et al., 2019) and will make spectrally more resolved UV data widely accessible. While atmospheric correction in the UV is difficult (Toratani et al., 2020), Vasilkov et al. (2019) report good results comparing observations with models. The improvement in the spectral resolution that will be available on PACE may lead to lower uncertainties in UV reflectance values, as well as improved resolution of different types of MAAs based on their spectral absorption signatures. Overall, this work demonstrates high potential for UV band ratio algorithms and lays the foundation for more advanced spectral approaches in discriminating the dominant phytoplankton group(s) within blooms based on MAA absorption signatures, greatly improving our ability to detect, monitor, and mitigate the impacts of different HAB species.

Recently, other researchers (Balch et al., 2018) have also observed the effects of MAA absorption on above-water reflectance (in the Atlantic Ocean using shipboard radiometry). While the $R_{rs}380/R_{rs}443$ ratios were employed in this study to detect and differentiate blooms of *L. polyedra* from diatom blooms, other dinoflagellates are also capable of synthesizing MAAs that absorb UV radiation overlapping with the 380 nm wave band, such as certain HAB members of the Alexandrium genus and other genera (Carreto et al., 2018). Future applications of UV remote sensing may be able to detect and separate different HAB species that produce high-biomass surface blooms across coastal regions worldwide.

4. Conclusions

A method of detecting dinoflagellate blooms proposed over two decades ago (Kahru and Mitchell, 1998) was implemented for the first time using newly available UV data from the SGLI sensor on the GCOM-C satellite and applied to an historic "red tide" event. The reduced ratio of $R_{rs}380/R_{rs}443$ was used as an indicator of dinoflagellate-dominated blooms and produced reasonable spatial and temporal patterns. However, more work is needed to validate the UV reflectance values and to associate different UV absorption patterns to different phytoplankton groups. More detailed ocean UV reflectance from PACE will require support for more detailed UV in situ and laboratory observations together with MAA and other optically important constituents to allow more advanced algorithm development that may allow remote discrimination of different phytoplankton taxa. This methodology has exciting potential to monitor the formation and fate of a key harmful algal taxon that blooms episodically along the Southern California coast and elsewhere.

Data accessibility statement

Imaging FlowCytobot images and image products are available at https://ifcb-data.whoi.edu/SIO_Delmar_mooring. Merged satellite chlorophyll-a data are available at http://spg-satdata.ucsd.edu/ca1km/. Second-Generation Global Imager (SGLI) Level 2 are available at Japan Aerospace Exploration Agency's G-Portal website: https://gportal.jaxa.jp/gpr/. Composited SGLI data are available at http://spg-satdata.ucsd.edu/composited_SGLI_data/. All Scripps Pier phytoplankton data are available at https://sccoos.org/harmful-algal-bloom/.

Acknowledgments

Drs. Hiroshi Murakami and Kazunori Ogata of the Japan Aerospace Exploration Agency (JAXA) are gratefully acknowledged for giving access to the prerelease Second-Generation Global Imager data. Satellite data were provided by JAXA, the NASA Ocean Color Processing Group, ESA MERIS, and Sentinel programs. We thank Alexi Shalapyonok for expert assistance with Imaging FlowCytobot operation on the Del Mar mooring. We wish to specifically acknowledge K. Seech for her efforts with Scripps Pier sampling and phytoplankton cell identification and enumeration.

Funding

Part of this work was funded by National Science Foundation (NSF) grants to the CCE-LTER Program, most recently OCE-1637632. Processing of Second-Generation Global Imager satellite data was funded by Japan Aerospace Exploration Agency. Data shown in **Figure 1** were collected by BGM and MK with support from the NASA SIMBIOS project. DC was supported by the NASA Biodiversity and Ecological Forecasting Program (Grant NNX14AR62A), the Bureau of Ocean and Energy Management Ecosystem Studies Program (BOEM award MC15AC00006), and the NOAA through the Santa Barbara Channel Marine Biodiversity Observation Network. HMS was supported by NSF (Grant OCE-1810927) and the Simons Foundation (Grant 561126). ELW was supported by NSF GRFP (Grant DGE-1650112). Funding for Scripps and Santa Monica Piers sampling was through the Southern California Coastal Ocean Observing Harmful Algal Bloom Monitoring Program by NOAA NA16NOS0120022.

Competing interests

The authors have declared that no competing interests exist.

Author contributions

Contributed to conception and design: MK, CA, ELW, BGM.

Contributed to acquisition of data: MK, ADB, MLC, DC, US, HMS.

Contributed to analysis and interpretation of data: MK, ADB, MLC, DC, US, HMS, ELW.

Drafted and/or revised this article: MK, CA, ADB, MLC, DC, US, HMS, ELW, BGM.

Approved the submitted version for publication: MK, CA, ADB, MLC, DC, US, HMS, ELW, BGM.

References

Allen, WE. 1938. "Red Water" along the West Coast of the United States in 1938. *Science* **88**(2272): 55–56.

Anderson, CR, Brzezinski, MA, Washburn, L, Kudela, R. 2006. Circulation and environmental conditions during a toxigenic *Pseudo-nitzschia australis* bloom in the Santa Barbara Channel, California. *Marine Ecology Progress Series* **327**: 119–133.

Anderson, CR, Siegel, DA, Brzezinski, MA, Guillocheau, N. 2008. Controls on temporal patterns in phytoplankton community structure in the Santa Barbara Channel, California. *Journal of Geophysical Research* **113**(C4): 140.

Balch, W, Drapeau, D, Bowler, B, Mitchell, C. 2018. Persistent UV reflectance peaks in the Gulf of Maine observed using above-water, hyperspectral radiometry: New observations from the Gulf of Maine North Atlantic Time Series (GNATS), Ocean Optic XXIV, Dubrovnik, Croatia. Available at https://oceanopticsconference.org/abstracts/balch.pdf. Accessed 1 October 2020.

Barrón, RK, Siegel, DA, Guillocheau, N. 2014. Evaluating the importance of phytoplankton community structure to the optical properties of the Santa Barbara Channel, California. *Limnology and Oceanography* **59**(3): 927–946.

Barth, A, Walter, RK, Robbins, I, Pasulka, A. 2020. Seasonal and interannual variability of phytoplankton abundance and community composition on the Central Coast of California. *Marine Ecology Progress Series* **637**: 29–43.

Carreto, JI, Carignan, MO, Montoya, NG, Cozzolino, E, Akselman, R. 2018. Mycosporine-like amino acids and xanthophyll-cycle pigments favour a massive spring bloom development of the dinoflagellate *Prorocentrum minimum* in Grande Bay (Argentina), an ozone hole affected area. *Journal of Marine Systems* **178**: 15–28.

Catlett, D, Siegel, DA. 2018. Phytoplankton pigment communities can be modeled using unique relationships with spectral absorption signatures in a dynamic coastal environment. *Journal of Geophysical Research: Oceans* **123**(1): 246–264.

Catlett, D, Siegel, DA, Simons, RD, Guillocheau, N, Henderikx-Freitas, F, Thomas, CS. n.d. Diagnosing seasonal to multi-decadal phytoplankton group dynamics in a highly productive coastal ecosystem. *Progress Oceanography*, in press.

Fischer, AD, Hayashi, K, McGaraghan, A, Kudela, RM. 2020. Return of the "age of dinoflagellates" in Monterey Bay: Drivers of dinoflagellate dominance examined using automated imaging flow cytometry and long-term time series analysis. *Limnology and Oceanography* **65**(9): 2125–2141.

Goericke, R. 2011. The structure of marine phytoplankton communities-patterns, rules, and mechanisms. *California Cooperative Oceanic Fisheries Investigations Report* **52**: 182–197.

Goodman, D, Eppley, RW, Reid, FMH. 1984. Summer phytoplankton assemblages and their environmental correlates in the Southern California Bight. *Journal of Marine Research* **42**(4): 1019–1049.

Harms, S, Winant, CD. 1998. Characteristic patterns of the circulation in the Santa Barbara Channel. *Journal of Geophysical Research* **103**(C2): 3041–3065.

Hatch, MBA, Schellenberg, SA, Carter, ML. 2013. Ba/Ca variations in the modern intertidal bean clam *Donax gouldii*. An upwelling proxy? *Palaeogeography, Palaeoclimatology, Palaeoecology* **373**: 98–107. DOI: https://dx.doi.org/10.1016/j.palaeo.2012.03.006.

Henderikx Freitas, F, Siegel, DA, Maritorena, S, Fields, E. 2017. Satellite assessment of particulate matter and phytoplankton variations in the Santa Barbara Channel and its surrounding waters: Role of surface waves. *Journal of Geophysical Research: Oceans* **122**(1): 355–371.

Jester, R, Lefebvre, K, Langlois, G, Vigilant, V, Baugh, K, Silver, MW. 2009. A shift in the dominant toxin-producing algal species in central California alters phycotoxins in food webs. *Harmful Algae* **8**(2): 291–298.

Kahru, M, Mitchell, BG. 1998. Spectral reflectance and absorption of a massive red tide off southern California. *Journal of Geophysical Research* **103**(C10): 21601–21609.

Kudela, RM, Bickel, A, Carter, ML, Howard, MDA, Rosenfeld, L. 2015. Chapter 5, The monitoring of harmful algal blooms through ocean observing: The development of the California Harmful Algal Bloom Monitoring and Alert Program, in Liu, Y, Kerkering, H, Weisberg, RH eds., *Coastal Ocean observing systems*. Boston, MA: Academic Press: 58–75.

Mantyla, AW, Bograd, SJ, Venrick, EL. 2008. Patterns and controls of chlorophyll-a and primary productivity cycles in the Southern California Bight. *Journal of Marine Systems* **73**(1): 48–60.

Mitchell, BG, Kahru, M. 2009. Bio-optical algorithms for ADEOS-2 GLI. *Journal of the Remote Sensing Society of Japan* **29**(1): 80–85.

Moisan, TA, Mitchell, BG. 2001. UV absorption by mycosporine-like amino acids in *Phaeocystis antarctica* Karsten induced by photosynthetically available radiation. *Marine Biology* **138**(1): 217–227.

Murakami, H. 2020. ATBD of GCOM-C chlorophyll-a concentration algorithm. JAXA, EORC. Available at https://suzaku.eorc.jaxa.jp/GCOM_C/data/ATBD/ver2/V2ATBD_O3AB_Chla_Murakami.pdf. Accessed 3 October 2020.

Olson, RJ, Sosik, HM. 2007. A submersible imaging-in-flow instrument to analyze nano-and microplankton: Imaging FlowCytobot. *Limnology and Oceanography: Methods* **5**(6): 195–203.

Otero, MP, Siegel, DA. 2004. Spatial and temporal characteristics of sediment plumes and phytoplankton

blooms in the Santa Barbara Channel. *Deep Sea Research Part II: Topical Studies in Oceanography* **51**(10): 1129–1149.

Shick, JM, Dunlap, WC. 2002. Mycosporine-like amino acids and related gadusols: Biosynthesis, accumulation, and UV-protective functions in aquatic organisms. *Annual Review of Physiology* **64**(1): 223–262. DOI: https://dx.doi.org/10.1146/annurev.physiol.64.081501.155802.

Sosik, HM, Futrelle, J, Brownlee, EF, Peacock, E, Crockford, T, Olson, RJ. 2020. IFCB-analysis software system code repository. Available at https://github.com/hsosik/ifcb-analysis/. Accessed 6 October 2020.

Sosik, HM, Olson, RJ. 2007. Automated taxonomic classification of phytoplankton sampled with imaging-in-flow cytometry. *Limnology and Oceanography: Methods* **5**(6): 204–216.

Stires, JC, Latz, MI. 2018. Contribution of the cytoskeleton to mechanosensitivity reported by dinoflagellate bioluminescence. *Cytoskeleton* **75**(1): 12–21.

Tanaka, K, Okamura, Y, Mokuno, M, Amano, T, Yoshida, J. 2018. First year on-orbit calibration activities of SGLI on GCOM-C satellite. *Earth Observing Missions and Sensors: Development, Implementation, and Characterization V* **10781**: 107810Q.

Taylor, AG, Landry, MR, Selph, KE, Wokuluk, JJ. 2015. Temporal and spatial patterns of microbial community biomass and composition in the Southern California Current Ecosystem. *Deep Sea Research Part II: Topical Studies in Oceanography* **112**: 117–128.

Toratani, M, Ogata, K, Fukushima, H. 2020. SGLI algorithm theoretical basis document: Atmospheric correction algorithm for ocean color. Version 2. JAXA, EORC. Available at https://suzaku.eorc.jaxa.jp/GCOM_C/data/ATBD/ver2/V2ATBD_O2AB_NWLR_Toratani_jp.pdf. Accessed 2 October 2020.

Vasilkov, A, Lyapustin, A, Mitchell, BG, Huang, D. 2019. UV reflectance of the ocean from DSCOVR/EPIC: Comparisons with a theoretical model and Aura/OMI observations. *Journal of Atmospheric and Oceanic Technology* **26**(1): 2087–2099.

Venrick, EL. 2002. Floral patterns in the California Current System off southern California: 1990–1996. *Journal of Marine Research* **60**(1): 171–189.

Vernet, M, Whitehead, K. 1996. Release of ultraviolet-absorbing compounds by the red-tide dinoflagellate *Lingulodinium polyedra*. *Marine Biology* **127**(1): 35–44.

Werdell, PJ, Behrenfeld, MJ, Bontempi, PS, Boss, E, Cairns, B, Davis, GT, Franz, BA, Gliese, UB, Gorman, ET, Hasekamp, O, Knobelspiesse, KD, Mannino, A, Martins, JV, McClain, CR, Meister, G, Remer, LA. 2019. The Plankton, Aerosol, Cloud, ocean Ecosystem mission: Status, science, advances. *Bulletin of the American Meteorological Society* **100**(9): 1775–1794.

Whitehead, K, Vernet, M. 2000. Influence of mycosporine-like amino acids (MAAs) on UV absorption by particulate and dissolved organic matter in La Jolla Bay. *Limnology and Oceanography* **45**(8): 1788–1796.

How to cite this article: Kahru, M, Anderson, C, Barton, AD, Carter, ML, Catlett, D, Send, U, Sosik, HM, Weiss, EL, Mitchell, BG. 2021. Satellite detection of dinoflagellate blooms off California by UV reflectance ratios. *Elementa: Science of the Anthropocene* 9(1). DOI: https://doi.org/10.1525/elementa.2020.00157

Domain Editor-in-Chief: Jody W. Deming, University of Washington, Seattle, WA, USA

Associate Editor: Kevin Arrigo, Department of Earth System Science, Stanford University, Stanford, CA, USA

Knowledge Domain: Ocean Science

Part of an Elementa Special Feature: Red Tide: Multidisciplinary Studies of an Exceptional Algal Bloom in Southern California

Published: June 9, 2021 **Accepted:** May 13, 2021 **Submitted:** October 15, 2020

ELEMENTA Science of the Anthropocene

Elem Sci Anth is a peer-reviewed open access journal published by University of California Press.

OPEN ACCESS